

Engineering Notes

ENGINEERING NOTES are short manuscripts describing new developments or important results of a preliminary nature. These Notes cannot exceed 6 manuscript pages and 3 figures; a page of text may be substituted for a figure and vice versa. After informal review by the editors, they may be published within a few months of the date of receipt. Style requirements are the same as for regular contributions (see inside back cover).

Influence of Scattering on Infrared Signatures of Rocket Plumes

H. F. Nelson*

University of Missouri-Rolla, Rolla, Missouri

Introduction

SOLID propellant tactical rocket exhaust plumes contain particles that significantly influence their radiation emission characteristics. In order to improve infrared (IR) signature predictions, JANNAF (Joint Army-Navy-NASA-Air Force) recently developed a Standard Plume Model, which consists of a Standard Plume Flowfield (SPF)¹⁻³ and a Standard Infrared Radiation Model (SIRRM).⁴⁻⁹

The SPF code predicts rocket exhaust plume flowfield structure at low (0-70 km) altitudes. The current version of SPF does not account for two-phase plumes; however, it calculates the mole fraction of particle molecules at each flowfield point (r, z), which can be converted to a number density of particles at a specific size.⁷⁻⁹ Because of this limitation, heat and mass transfer between the particles and the gases are not accounted for.

The SIRRM code calculates the infrared radiation signature of exhaust plumes. It considers multiple scattering, emission, and absorption processes in a rigorous, but computationally tractable, approach as a function of axial and radial position in the plume. The code contains options for different degrees of sophistication in treating particulate scattering (pseudogas, two-flux, and six-flux). It also contains an up-to-date data base for aluminum oxide, carbon, magnesium oxide, and zirconium oxide particles, and 26 IR active gases in the 2- to 25- μm spectral range.

SIRRM has been validated by comparing its output with well-documented experimental results. The agreement with static cases was usually much better than the SIRRM design guideline of factor-of-two accuracy. The agreement with gas-dynamic cases was not as good, probably because of insufficient accuracy in the flowfield description.⁵

Analysis

The equation for radiative transfer along a line of sight in the direction of vector, s , is

$$\frac{dI_\omega(s)}{ds} = -\beta_\omega I_\omega(s) + \sum_{j=1}^J \left[K_{\omega,j} I_{b\omega,j}(s) + \frac{\gamma_{\omega,j}}{4\pi} \int_{4\pi} I_\omega(s') P_{\omega,j}(s',s) d\Omega(s') \right] \quad (1)$$

in which $I_\omega(s)$ is the spectral radiance at point s at wavenumber ω in the direction s , and j is a subscript that represents the species. The phase function for scattering from direction s' to direction s is denoted by $P_{\omega,j}(s',s)$. The term $I_{b\omega,j}(s)$ represents the blackbody spectral radiance at point s . It is a function of j because the temperature may be different for each gaseous or particle species. The scattering coefficient is

$$\gamma_\omega = \sum_{j=1}^J \gamma_{\omega,j} = \sum_{j=1}^J N_j \sigma_{\omega,j}^s \quad (2)$$

in which N_j is the number density and $\sigma_{\omega,j}^s$ is the scattering cross section of species j . The absorption coefficient is

$$K_\omega = \sum_{j=1}^J K_{\omega,j} = \sum_{j=1}^J N_j \sigma_{\omega,j}^a \quad (3)$$

where $\sigma_{\omega,j}^a$ is the absorption cross section of species j . Thus, the extinction coefficient becomes $\beta_\omega = \gamma_\omega + K_\omega$.

The first term on the right side of Eq. (1) represents the radiation lost from the line of sight as a result of absorption and scattering. The second term denotes the emission at point s , and the third term accounts for the radiation from all other directions, s' , that is scattered into the line of sight. SIRRM simplifies the integral term of Eq. (1) by using models for the scattering phase function. The gas-only model neglects all particle effects. The pseudogas model sets $\sigma_{\omega,j}^s$ equal to zero; however, it allows for the contribution of particles and gases to $\sigma_{\omega,j}^a$. The two-flux and six-flux models assume the scattering phase function consists of two components (forward and backward) and six components (forward, backward, and each of four sides), respectively. The radiative emission from the plume is obtained using a finite difference numerical scheme.

Plume Flowfield

The infrared spectrum was predicted for a representative aluminized composite propellant (16% aluminum in propellant by weight) using SPF and SIRRM. The calculations were made for conditions at sea-level and at 6.1 km for a Mach 2 rocket plume with an exit diameter of 10 cm and a mass flow rate of 5.9 kg/s. The rocket nozzle exit conditions were predicted using a one-dimensional nozzle flow analysis for the assumption that chemical equilibrium existed in the combustion chamber and nozzle. The mole fractions at the nozzle exit were: $\text{Al}_2\text{O}_3 = 0.07$, $\text{CO} = 0.30$, $\text{CO}_2 = 0.004$, $\text{H}_2 = 0.41$, $\text{H}_2\text{O} = 0.02$, $\text{HCl} = 0.13$ and $\text{N}_2 = 0.07$. At the nozzle exit the pressure was 123.6 kPa (1.22 atm), the temperature was 1860 K and the velocity was 2.5 km/s. Figure 1 shows the plume centerline temperatures and concentrations for the sea-level and 6.1-km altitude plumes as a function of distance from the nozzle exit. The plumes undergo afterburning as indicated by the strong temperature rise, the local maximums in the H_2O and CO_2 centerline concentrations, and the rapid reduction of the CO mole fraction as a function of axial position. The plumes have a high Al_2O_3 particle mole fraction because of the large aluminum mass fraction in the propellant. Note the jump in temperature near the nozzle exit due to shockwaves and that

Submitted July 25, 1983; revision received Sept. 28, 1983. Copyright © American Institute of Aeronautics and Astronautics, Inc., 1983. All rights reserved. Copyright © American Institute of Aeronautics and Astronautics, Inc., 1983. All rights reserved.

*Professor of Aerospace Engineering, Thermal Radiative Transfer Group, Department of Mechanical & Aerospace Engineering, Associate Fellow AIAA.

the maximum temperature for the sea-level plume is slightly higher than it is for the 6.1-km plume.

Plume Radiation Signatures

To investigate the effect of scattering, the mole fraction of Al_2O_3 was converted to particles of a specific size, and the broadside radiative emission was calculated using the four radiation scattering models: gas-only, pseudogas, two-flux, and six-flux.⁷ The atmosphere between the plume and observer was assumed to have a transmissivity of unity.

Figure 2 shows the broadside, station radiation for the plume in the 2000 to 5000 $1/\text{cm}$ wavenumber spectral band. It shows the pseudogas and six-flux signatures for the plumes containing 0.1-, 1.0-, and 10.0- μm diameter aluminum oxide particles in terms of axial position. The gas-only and the two-flux results were essentially the same as the pseudogas results, so they are not shown.

In general, the radiation increases with axial distance near the nozzle exit and reaches a maximum in the afterburning region, because of the increase in the concentration of CO_2 and H_2O and the temperature due to afterburning. Most of the plume infrared signature is emitted in the CO , CO_2 , and H_2O gaseous bands. These gases attain relatively high concentrations and temperatures in the afterburning zone. The radiation begins to decrease downstream from the afterburning region because of the entrainment of cold air. This cools the plume and consequently reduces the emissive power of the gaseous bands.

The influence of scattering and aluminum oxide particle size is shown in Fig. 2 as the difference between the six-flux and pseudogas solutions. The pseudogas solutions are essentially independent of particle size. Scattering increases the radiation, especially in the near-plume and afterburning regions for plumes with 1.0- and 10.0- μm particles. The magnitude of the peak station radiation is about the same for sea-level and 6.1-km plumes.

Figure 3 shows the radiant intensity of the plumes in the 2000 to 5000 $1/\text{cm}$ wavenumber band for each particle size in terms of the radiation scattering model used in the calculation. The height of each bar represents the area under a specific curve, like those shown in Fig. 2.

The gas-only and pseudogas models yield approximately the same magnitude for IR intensity because the Al_2O_3 particles have very small absorption coefficients in the 2000 to 5000 $1/\text{cm}$ wavenumber band and, hence, low emission.

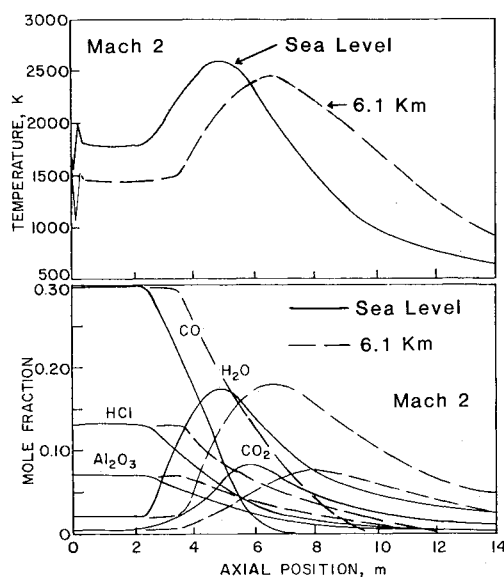


Fig. 1 Centerline temperature and species concentration vs axial position for the sea-level and 6.1-km altitude, Mach 2 plumes.

Thus, the IR signature is similar if one neglects the Al_2O_3 particles, or if one considers only their absorption/emission.

The two-flux model predicts intensity magnitudes that are roughly the same as those of the pseudogas model. The two-flux results are somewhat sensitive to particle size, with the plumes containing 1.0- μm particles emitting the largest intensity.

The signatures predicted using the six-flux model are sensitive to particle size. The results for plumes with 0.1- μm particles are about the same as those for the pseudogas and two-flux models for all particle sizes. However, increasing the particle size to 1.0 μm increases the emission by approximately 33%. Increasing the particle size further to 10.0 μm causes the emission to decrease from its 1.0- μm particle value. The sensitivity to particle size is mainly due to the side-scattering effectiveness of the particles, which turns the optically thick axially directed radiation to the less optically thick radial direction.⁷ The side-scattering is a function of

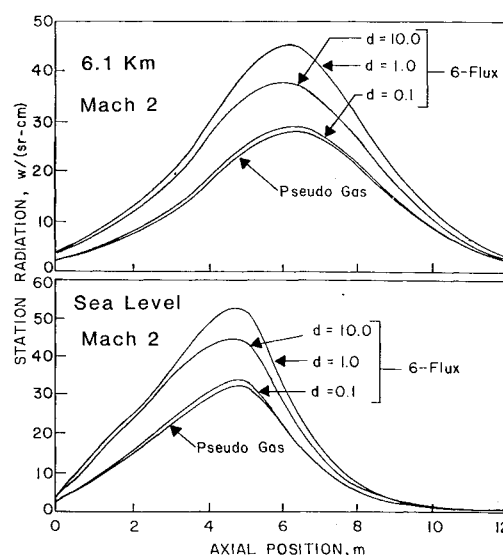


Fig. 2 Six-flux and pseudogas broadside station radiation vs axial position for the sea-level and 6.1-km altitude, Mach 2 plumes.

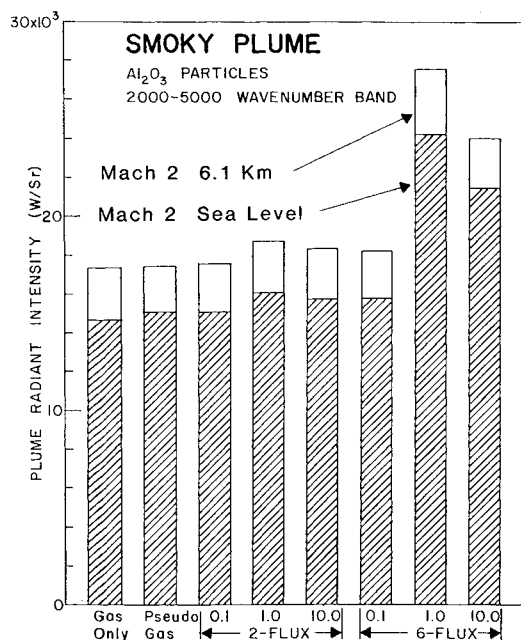


Fig. 3 Comparisons of the plume radiant intensity in the 2000 to 5000 $1/\text{cm}$ wavenumber band.

$\sigma_{\omega,j}^s$ and $P_{\omega,j}(s,s')$, which depend on particle size. The radiant intensity from plumes at an altitude of 6.1 km is about 20% larger than from plumes at sea-level because the temperatures of the former remain higher over a longer distance along the plume and because the plumes are slightly larger.

Conclusions

The following conclusions on the influence of scattering on IR signatures of realistic rocket plumes can be drawn from the numerical results presented herein.

1) The IR signature of rocket plumes is sensitive to radiation scattering. The six-flux solutions are more realistic and are more sensitive to scattering than gas-only, pseudogas, and two-flux solutions because the six-flux model considers scattering into and out of the line of sight.

2) The effect of scattering is a function of particle size. Particles with diameters near 1.0- μm influence the broadside signature more than smaller or larger particles.

3) High altitude plumes emit larger IR signatures than sea-level plumes for the same nozzle exit conditions. This occurs mainly because they are larger.

4) Al_2O_3 is a weak absorber/emitter in the 2000-5000 $1/\text{cm}$ wavenumber band; consequently the source of the plume signature is due to gas emission. Particle scattering influences the signature by changing its directional pattern.¹⁰

In terms of modeling, this study shows a strong need for accurate determination of the particle size as a function of position throughout the plume for accurate signature predictions. The six-flux model, which is the most realistic of the scattering models considered herein, predicts a strong sensitivity of the signature magnitude to the particle size.

References

- 1 Dash, S. M., Pergament, H. S., and Thorpe, R. D., "The JANNAF Standard Plume Flowfield Model: Modular Approach, Computational Features and Preliminary Results," *Joint Army-Navy-NASA-Air Force (JANNAF) 11th Plume Technology Meeting Proceedings*, Chemical Propulsion Information Agency (CPIA) Publication 306, July 1979, pp. 345-442.
- 2 Dash, S. M. and Pergament, H. S., "The JANNAF Standard Plume Flowfield Model: Operational Features and Preliminary Assessment," *Joint Army-Navy-NASA-Air Force (JANNAF) 12th Plume Technology Meeting Proceedings*, Vol. II, Chemical Propulsion Information Agency, (CPIA) Publication 332, Dec. 1980, pp. 225-228.
- 3 Dash, S. M., Wolf, D. E., Beddini, R. A., and Pergament, H. S., "Analysis of Two-Phase Flow Processes in Rocket Exhaust Plumes," AIAA Paper 83-0248, 1983.
- 4 Ludwig, C. B., Malkmus, W., Walker, G. N., Reed, R., and Slack, M., "Standardized Infrared Radiation Model," AIAA Paper 81-1051, 1981.
- 5 Ludwig, C. B., Malkmus, W., Walker, J., Freeman, G. N., Reed, R., and Slack, M., "Standardized Infrared Radiation Model (SIRRM), Volume I: Development and Validation," Air Force Rocket Propulsion Laboratory AFRPL-TR-81-54, 1981.
- 6 Walker, J., Malkmus, W., and Ludwig, C. B., "Handbook of the Standardized Infrared Radiation Model (SIRRM), Volume I: Technical Manual, and Volume II: User's Manual," Air Force Rocket Propulsion Laboratory, AFRPL-TR-81-61, 1981.
- 7 Nelson, H. F., "Influence of Radiation Scattering on Infrared Signatures of Low Altitude Plumes," Air Force Rocket Propulsion Laboratory, AFRPL-TR-82-057, 1982.
- 8 Nelson, H. F., "Infrared Radiation Signatures of Tactical Rocket Exhausts," AIAA Paper 82-913, 1982.
- 9 Nelson, H. F., "Scattering of Infrared Radiation in Rocket Exhaust Plumes," *Proceedings Joint Army-Navy-NASA-Air Force (JANNAF) 13th Plume Technology Meeting Proceedings*, Chemical Propulsion Information Agency, (CPIA) Publication 357, April 1982, pp. 201-210.
- 10 Lyons, R. B., Wormhoudt, J., and Gruninger, J., "Scattering of Radiation by Particles in Low-Altitude Plumes," *Journal of Spacecraft and Rockets*, Vol. 20, March-April 1983, pp. 189-192.

Ultralight Reactive Metal Foams in Space: A Novel Concept

Franklin Hadley Cocks*

Duke University, Durham, North Carolina

LARGE-scale engineering projects increasingly have become a focus of attention in space development planning. Such projects typically would require much greater total payload tonnages than any undertaken previously. Therefore, the question of the density, strength, and stiffness of the materials chosen for use in such projects becomes of greatly increased importance. In current space activities, aluminum alloys are the materials of choice for most structural applications. Aluminum alloys are used in spite of the difference in densities of aluminum and magnesium (2.70 g/cm^3 vs 1.74 g/cm^3 , respectively), partly because the increased chemical activity of magnesium makes high-strength magnesium alloys much more susceptible than aluminum alloys to environmental degradation in the terrestrial environment. Additionally, the Young's modulus of magnesium (45 GPa, 6.5×10^6 psi) is significantly less than that of Al (70 GPa, 10×10^6 psi) and the maximum yield strengths of wrought Al alloys (e.g., 525 MPa, 76 ksi for 7175-T66) are substantially above those of wrought Mg alloys (e.g., 305 MPa, 44 ksi for ZK60A-T5). Both Mg and Al alloys are susceptible to stress corrosion cracking,¹ and more than one Apollo mission has been affected by the stress corrosion failure of aluminum alloy or titanium alloy components.^{2,4}

In large-scale space applications which do not involve crew quarters or other water- or oxygen-containing environments, as, for example, in solar power satellites, chemical reactivity is no longer as important as density, strength, and stiffness and the associated cost of transporting the required mass of structural materials to the desired orbit. A proposed solar power station might require 1000 metric tons of structural aluminum girders, but approximately only 500 metric tons of girders if Mg-Li alloys (1.35 g/cm^3) were substituted for aluminum alloys (2.70 g/cm^3). This reduction in payload mass might well be worth the additional difficulty of dealing with a more reactive material on Earth. As will be seen, there may, in fact, be an approach to the problem of the inherent reactivity of light metals which simultaneously ameliorates the problem of their low moduli of elasticity and makes their handling on Earth relatively straightforward.

Although there are certain exceptions, e.g., U and Pu, the relationship of increasing chemical reactivity with decreasing density appears to be generally true, as shown in Fig. 1. This figure shows the oxidation potential at unit activity⁵ plotted vs the density at 25°C⁶ of 25 metallic elements, including all those commonly used in alloys for terrestrial structural applications. Although the observed activity of certain elements, e.g., Al and Cr, is in practice lessened by the presence of passive adherent oxides, it is clear from this graph that as density decreases, reactivity increases. Thus Mg alloys are the lightest that can be used on Earth for any sort of structural application. All the elements lighter than Mg—that is, Ca, Na, K, and Li—have such great reactivities that they cannot be used themselves as structural materials on Earth. Because Li is very soluble in Mg,⁷ attempts have been made to develop Mg-Li alloys for structural purposes, and indeed such alloys

Received Jan. 12, 1984; revision received Feb. 13, 1984. Copyright © 1984 by F. H. Cocks. Published by the American Institute of Aeronautics and Astronautics, Inc., with permission.

*Professor, Department of Mechanical Engineering and Materials Science.